

((Fluoroformyl)imido)sulfonyl Difluoride, $\text{FC(O)N}=\text{S(O)F}_2$: Structural, Conformational, and Configurational Properties in the Gaseous and Condensed Phases

Roland Boese,[†] Edgardo H. Cutin,[‡] Rüdiger Mews,[§] Norma L. Robles,[‡] and Carlos O. Della Védova^{*,‡,‡,‡}

Institut für Anorganische Chemie, Universität GH Essen, Universitätsstrasse 5-7, D-45117 Essen, Germany, Instituto de Química Física, Facultad de Bioquímica, Química y Farmacia, Universidad Nacional de Tucumán, San Lorenzo 456, 4000 Tucumán, Argentina, CEQUINOR (UNLP-CONICET) and Laboratorio de Servicios a la Industria y al Sistema Científico (UNLP-CIC-CONICET), Departamento de Química, Facultad de Ciencias Exactas, Universidad Nacional de La Plata, 47 esq. 115, 1900 La Plata, Argentina, and Institut für Anorganische und Physikalische Chemie, Universität Bremen, 28334 Bremen, Germany

Received May 19, 2005

Structural, conformational, and configurational properties of the gaseous molecule ((fluoroformyl)imido)sulfonyl difluoride, $\text{FC(O)N}=\text{S(O)F}_2$, have been studied by vibrational spectroscopy (IR (gas) and Raman (liquid)) and quantum chemical calculations (HF, MP2, and B3LYP with 6-31+G* and 6-311+G* basis sets); in addition, the solid-state structure has been determined by X-ray crystallography. $\text{FC(O)N}=\text{S(O)F}_2$ exists in the gas phase as a mixture of a favored antiperiplanar–synperiplanar form (the S=O double bond antiperiplanar with respect to the C–N single bond, and the C=O group synperiplanar with respect to the S=N double bond) in equilibrium with less abundant antiperiplanar–antiperiplanar, synclinal–synperiplanar, and synclinal–antiperiplanar structures. The crystalline solid at 163 K (monoclinic, $P2_1/c$, $a = 5.1323(7)$ Å, $b = 15.942(2)$ Å, $c = 16.798(2)$ Å, $\beta = 95.974(3)^\circ$, $Z = 12$) consists of three similar antiperiplanar–synperiplanar forms.

Introduction

The approach to discussing covalent bonding in terms of shared pairs of electrons is attributable to G. N. Lewis, who in 1916 introduced this elementary but surprisingly successful idea.¹ The VSEPR (valence shell electron pair repulsion) method, also used in basic inorganic chemistry courses, is a simple extension of the Lewis formalism.² The prediction of molecular structures using either semiquantitative or sophisticated models is remarkable because chemical, spectroscopic, and photochemical properties and

reactivity can be often linked with molecular electronic structures.

((Fluoroformyl)imido)sulfonyl difluoride, $\text{FC(O)N}=\text{S(O)F}_2$, can be related to the known species $\text{FC(O)N}=\text{SF}_2$ ³ and O_2SF_2 .⁴ Formally removing the SF_2 group from the former molecule and one oxygen atom from the second results in the properly formed species $\text{FC(O)N}=\text{S(O)F}_2$. Whereas angles and bond distances can be successfully predicted from related molecules ($\text{NCN}=\text{S(O)F}_2$ ⁵ and $\text{FC(O)N}=\text{SF}_2$,³ for example), a prediction of the dihedral angles is much more complicated. In effect, this can be especially true for the $\text{O}=\text{S}=\text{N}-\text{C}$ torsion angle prediction in light of recent experimental and theoretical results for closely related molecules. Thus, whereas a cis–syn form is determined to

* To whom correspondence should be addressed. E-mail: carlosdv@quimica.unlp.edu.ar.

[†] Universität GH Essen.

[‡] Universidad Nacional de Tucumán.

[§] CEQUINOR (UNLP-CONICET), Universidad Nacional de La Plata.

[‡] Laboratorio de Servicios a la Industria y al Sistema Científico (UNLP-CIC-CONICET), Universidad Nacional de La Plata.

[‡] Universität Bremen.

(1) Lewis, G. N. *J. Am. Chem. Soc.* **1916**, *38*, 762–786.

(2) Gillespie, R. J.; Hargittai, I. *The VSEPR Model of Molecular Geometry*; Allyn and Bacon: Boston, 1991; pp 80–81.

(3) Leibold, Ch.; Cutin, E. H.; Della Védova, C. O.; Mack, H.-G.; Mews, R.; Oberhammer, H. *J. Mol. Struct.* **1996**, *375*, 207.

(4) Lide, D. R.; Mann, D. E.; Fristrom, R. M. *J. Chem. Phys.* **1957**, *26*, 734.

(5) Cutin, E. H.; Della Védova, C. O.; Mack, H.-G.; Oberhammer, H. *J. Mol. Struct.* **1995**, *354*, 165.

be the most stable one for the $\text{FC}(\text{O})\text{N}=\text{SF}_2$ molecule (the SF_2 bisector angle cis with respect to the $\text{C}-\text{N}$ bond, and the $\text{C}=\text{O}$ syn with respect to the $\text{N}=\text{S}$ bond), another form results for the closely related molecule $\text{FC}(\text{O})\text{N}=\text{S}(\text{F})\text{CF}_3$,⁶ which supposes a formal substitution of a F atom in $\text{FC}(\text{O})\text{N}=\text{SF}_2$ by a CF_3 group. For $\text{FC}(\text{O})\text{N}=\text{S}(\text{F})\text{CF}_3$, the main structure shows an antiperiplanar–synperiplanar form (antiperiplanar with respect to both lone pair orbitals at the N and S atoms, and the $\text{C}=\text{O}$ double bond synperiplanar with respect to the $\text{N}=\text{S}$ double bond).

We report here a structural, conformational, and configurational study of the title compound, drawing on its vibrational spectra, its single crystalline solid at 163 K, and quantum chemical calculations. The results will be compared with related species (OSF_2 ,⁷ O_2SF_2 ,⁴ $\text{HN}=\text{S}(\text{O})\text{F}_2$,⁸ $\text{CIN}=\text{S}^{\text{VI}}(\text{O})\text{F}_2$,⁹ $\text{NCN}=\text{S}(\text{O})\text{F}_2$,⁵ $\text{FC}(\text{O})\text{N}=\text{SF}_2$,³ and $\text{FC}(\text{O})\text{N}=\text{S}(\text{F})\text{CF}_3$) sequenced by using the Lewis formalism. This comparison also includes related previously reported compounds $\text{CF}_3\text{C}(\text{O})\text{N}=\text{S}(\text{F})\text{CF}_3$ ¹⁰ and $\text{FC}(\text{O})\text{N}=\text{SCL}_2$.¹¹

Quantum Chemical Calculations

Various forms of the molecule $\text{FC}(\text{O})\text{N}=\text{S}(\text{O})\text{F}_2$ are feasible, depending on the torsional position of the $\text{C}=\text{O}$ double bond around the $\text{N}-\text{C}$ single bond and on the orientation of the $\text{S}=\text{O}$ double bond relative to the $\text{N}-\text{C}$ single bond. The first orientation can be syn or anti [$\phi(\text{S}=\text{N}-\text{C}=\text{O}) = 0$ or 180°]. Geometry optimizations were performed with the program suite GAUSSIAN 98¹² for various fixed torsional angles $\phi(\text{S}=\text{N}-\text{C}=\text{O})$ around the $\text{C}-\text{N}$ bond, using the HF approximation and the hybrid method B3LYP with 6-31+G* basis sets. The resulting potential function for internal rotation possesses minima for the synperiplanar [$\phi(\text{S}=\text{N}-\text{C}=\text{O}) = 0^\circ$] and antiperiplanar [$\phi(\text{S}=\text{N}-\text{C}=\text{O}) = 180^\circ$] positions that are antiperiplanar to the fixed torsional angle around the $\text{S}=\text{N}$ double bond with $\phi(\text{O}=\text{S}=\text{N}-\text{C}) = 180^\circ$. Both antiperiplanar–synperiplanar (**I**) and antiperiplanar–antiperiplanar (**II**) forms lead to structures without imaginary vibrational frequencies (Scheme 1). Subsequently, another optimization was made for various fixed dihedral angles $\phi(\text{O}=\text{S}=\text{N}-\text{C})$ around the $\text{N}=\text{S}$ double bond that fixed the torsional angle $\phi(\text{S}=\text{N}-\text{C}=\text{O})$ at 0 and 180° .

Thus, two more stable forms around the $\text{N}=\text{S}$ appear to exist for this molecule. Thus the synclinal–synperiplanar (**III**) and

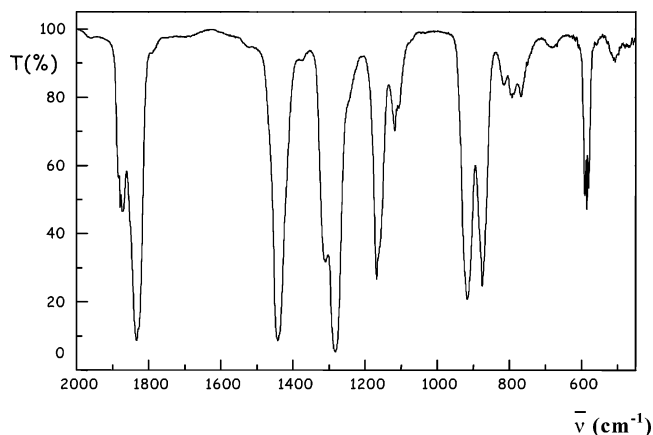
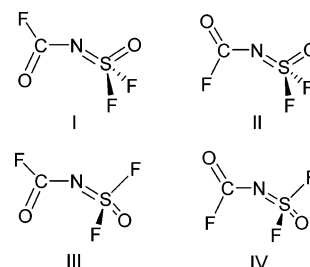


Figure 1. Room temperature infrared spectrum of $\text{FC}(\text{O})\text{N}=\text{S}(\text{O})\text{F}_2$ at 2.9 mbar (optical path 10 cm).

Scheme 1



synclinal–antiperiplanar (**IV**) forms represent minima in the energy hypersurface without any negative frequency (Scheme 1). Computational methods predict the structure **I** to be more stable than the structures **II**, **III**, and **IV**, with differences in ΔE^0 and ΔG^0 varying from 1.21 to 4.32 and 0.67 to 2.98 kcal mol⁻¹, respectively.

Despite the fact that some dispersion in the results becomes evident, computational methods are also in agreement about the fact that the four forms might be present together in principle with detectable quantities in the gas phase at ambient temperatures.

Vibrational Spectra

The IR spectrum of gaseous $\text{FC}(\text{O})\text{N}=\text{S}(\text{O})\text{F}_2$ and the Raman spectrum of the liquid are shown in Figures 1 and 2. Details of the spectra are itemized in Table 1, together with the wavenumbers calculated using theoretical calculations.

Information about the conformational properties is most easily derived from the IR spectra with the enhanced definition of vibrational features that they afford. It is well-known that the $\nu(\text{C}=\text{O})$ mode in $\text{XC}(\text{O})\text{N}=\text{S}$ -containing compounds shifts by about 30–50 cm⁻¹ when the $\text{C}=\text{O}$ bond is rotated from the synperiplanar to the antiperiplanar orientation relative to the $\text{S}=\text{N}$ bond. The synperiplanar orientation gives the lower wavenumber, with the weakening of the $\text{C}=\text{O}$ bond reflecting the orbital interaction between the n_σ lone pair orbital of the nitrogen with the $\sigma^*(\text{C}=\text{O})$ antibonding orbital (the anomeric effect).

The assignment of the bands at 1879 and 1833 cm⁻¹ in the gas IR spectrum (Figure 1) is straightforward. According to the calculations, the $\nu(\text{C}=\text{O})$ mode shows a small shift with the switch from synperiplanar to antiperiplanar orientation of $\text{C}=\text{O}$ relative to the $\text{N}=\text{S}$ group. This shift was

- (6) Trautner, F.; Cutin, E. H.; Della Védova, C. O.; Mews, R.; Oberhammer, H. *Inorg. Chem.* **2000**, *39*, 4833.
 (7) Lucas, N. J. D.; Smith, J. G. *J. Mol. Spectrosc.* **1972**, *43*, 327.
 (8) Cassoux, P.; Kuczowski, R. L.; Creswell, R. A. *Inorg. Chem.* **1977**, *16*, 2959.
 (9) Oberhammer, H.; Glemser, O.; Klüver, H. *Z. Naturforsch.* **1974**, *29a*, 901.
 (10) Hermann, A.; Mora Valdez, M. I.; Cutin, E. H.; Della Védova, C. O.; Oberhammer, H. *J. Phys. Chem. A* **2003**, *107*, 7874.
 (11) Leibold, Ch.; Alvarez, R. S. M.; Cutin, E. H.; Della Védova, C. O.; Oberhammer, H. *Inorg. Chem.* **2003**, *42*, 4071.
 (12) Frisch, M. J.; Trucks, G. W.; Schlegel, H. B.; Scuseria, G. E.; Robb, M. A.; Cheeseman, J. R.; Zakrzewski, V. G.; Montgomery, J. A., Jr.; Stratmann, R. E.; Burant, J. C.; Dapprich, S.; Millam, J. M.; Daniels, A. D.; Kudin, K. N.; Strain, M. C.; Farkas, O.; Tomasi, J.; Barone, V.; Cossi, M.; Cammi, R.; Mennucci, B.; Pomelli, C.; Adamo, C.; Clifford, S.; Ochterski, J.; Petersson, G. A.; Ayala, P. Y.; Cui, Q.; Morokuma, K.; Malick, D. K.; Rabuck, A. D.; Raghavachari, K.; Foresman, J. B.; Cioslowski, J.; Ortiz, J. V.; Baboul, A. G.; Stefanov, B. B.; Liu, G.; Liashenko, A.; Piskorz, P.; Komaromi, I.; Gomperts, R.; Martin, R. L.; Fox, D. J.; Keith, T.; Al-Laham, M. A.; Peng, C. Y.; Nanayakkara, A.; Gonzales, C.; Challacombe, M.; Gill, P. M. W.; Johnson, B.; Chen, W.; Wong, M. W.; Andres, J. L.; Head-Gordon, M.; Replogle, E. S.; Pople, J. A. *Gaussian 98*, revision A.7; Gaussian, Inc.: Pittsburgh, PA, 1998.

Table 1. Vibrational Data for FC(O)N=S(O)F₂^d

antiperiplanar- synperiplanar ^b	synclinal- synperiplanar ^b	antiperiplanar- antiperiplanar ^b	antiperiplanar- synperiplanar ^c	antiperiplanar- antiperiplanar ^c	antiperiplanar- synperiplanar ^c	synclinal- synperiplanar ^c	antiperiplanar- antiperiplanar ^d	antiperiplanar- synperiplanar ^d	antiperiplanar- antiperiplanar ^d	IR ^e (gas) (3 mbar)	Raman (liquid)	assignment ^e
I	III	II	I	II	I	III	I	II	II			
		1901		1914			1911			1884	1853	ν (C=O)
1842	1839		1871	1867	1872	1864				1879		
1380	1364	1394	1386	1363	1454	1430	1462			1833	1819	ν (C=O)
1307	1306	1294	1255	1253	1300	1291	1316			1827		
1164	1165		1131	1134	1165	1166				1442	1441	ν_{as} (NSO) ν_{as} (NSO)
		1129					1106			1436		
922	913	875	880	869	907	901	833			1310	1307	ν_s (NSO)
880	899	869	772	811	792	839	784			1282	1274	ν_s (NSO)
803	824	781	766	766	775	775	745			1168	1169	ν (C-F)
788	781		711	730	732	750				1164		
							1106			1118	1149	ν (C-F)
										1111		
										1107		
										916	918	δ_s (SOF ₂)
										876	885	δ_s (SOF ₂)
										815	852	ν_{as} (SF ₂)
										797	817	ν_{as} (SF ₂)
										792	794	ν (C-N)
										787		
										768	692	ν (C-N)
										681		γ (FCO)
										590	584	γ (FCO)
										585		δ (FCO)
										580		
										506		δ (FCO)
										500		δ (SOF ₂)
										468		δ (SOF ₂)
										436		δ (SOF ₂)
										404		δ (SOF ₂)
										395		δ (SOF ₂)
										367		δ (SOF ₂)
										356		δ (SOF ₂)
										341		δ (SOF ₂)
										325		δ (SF ₂)
										143	136	δ (CNS)
										96		torsion
										43		torsion
										37		torsion

^a Wavenumbers are in cm⁻¹. ^b Scaled by a factor of 0.9; the HF/6-31+G* basis set was used. ^c The B3LYP/6-311+G* basis set was used. ^d The MP2/6-311+G* basis set was used. ^e A band contour is determined. ^f ν = stretching, δ = deformation, γ = out-of-plane deformation, s = symmetric and as = antisymmetric.

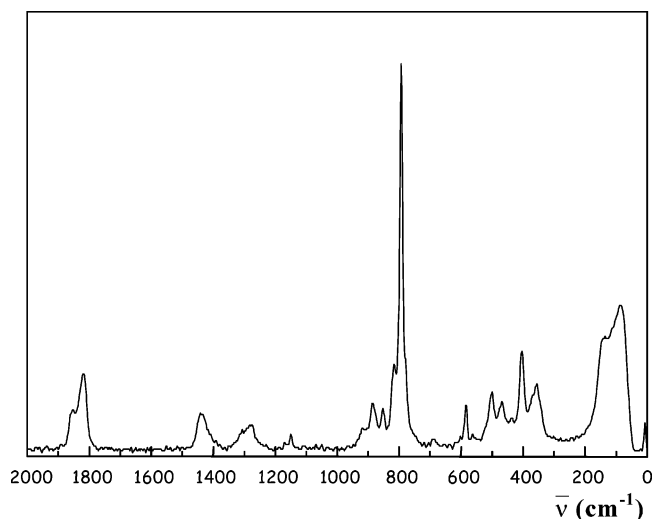


Figure 2. Raman spectrum of FC(O)N=S(O)F₂ liquid at room temperature, taken with the 1064 nm excitation line (150 mW, resolution 4 cm⁻¹).

Table 2. Crystal Data and Structure Refinement for FC(O)N=S(O)F₂

empirical formula	CF ₃ NO ₂ S
fw (Da)	147.08
<i>d</i> _{calcd} (g cm ⁻³)	2.144
<i>F</i> (000)	864
<i>T</i> (K)	163(2)
cryst size (mm)	0.3
cryst color	colorless
cryst description	cylindrical
wavelength (Å)	0.71073
cryst syst	monoclinic
space group	<i>P</i> 2 ₁ / <i>c</i>
<i>a</i> (Å)	5.1323(7)
<i>b</i> (Å)	15.942(2)
<i>c</i> (Å)	16.798(2)
α (deg)	90
β (deg)	95.974(3)
γ (deg)	90
<i>V</i> (Å ³)	1366.9(3)
<i>Z</i>	12
no. of cell measurement reflns used	3884
cell measurement θ min/max (deg)	2.44–28.28
θ range (deg)	2.44–28.29
completeness to θ = 28.29° (%)	68.5
index ranges	−4 ≤ <i>h</i> ≤ 3, −21 ≤ <i>k</i> ≤ 21, −16 ≤ <i>l</i> ≤ 22
abs coeff (mm ⁻¹)	0.687
max/min transmission	1.00/0.88
<i>R</i> _(merg) before/after correction	0.0443/0.0146
no. of reflns collected	5410
no. of independent reflns	2324 [<i>R</i> _(int) = 0.0150]
data/restraints/parameters	2042/0/218
GOF on <i>F</i> ²	1.034
final <i>R</i> indices [<i>I</i> > 2σ(<i>I</i>)]	<i>R</i> ₁ = 0.0249, <i>wR</i> ₂ = 0.0685 ^a
<i>R</i> indices (all data)	<i>R</i> ₁ = 0.0290, <i>wR</i> ₂ = 0.0723 ^a
extinction coeff	0.0054(8)
largest diff. peak and hole (e Å ⁻³)	0.311, −0.262

$$^a w = 1/[\sigma^2(F_o^2) + (0.0417P)^2 + 0.486P], \text{ where } P = (F_o^2 + 2F_c^2)/3.$$

calculated to be in the range 39–59 cm⁻¹, according to the levels of approximation used (Tables 1 and 3). A third band can be observed at 1827 cm⁻¹. According to the predicted normal modes of vibration, this band might have originated from the synclinal–synperiplanar form (**III**). The calculated IR absorption coefficients are also very similar for the three forms. On the basis of the calculated free energies, we plausibly assign the strongest band centered at 1833 cm⁻¹ to form **I**, the band centered at 1879 cm⁻¹ to form **II**, and

the band at 1827 cm⁻¹ to form **III**. Moreover, the 1884 cm⁻¹ band might be assigned to the C=O vibration of the less stable form **IV**, according to the vibrational trend calculated from computational chemistry. Its feasible origin as a derivative from a band contour of the band centered at 1879 cm⁻¹ or as a combination band cannot be ruled out.

From the integrated areas of the two subgroups of bands (**I** and **III**, **II** and **IV**), and without any correction from calculated IR absorption coefficients, a contribution of 15(5)% could be derived for the forms **II** and **IV** with an error limit based on the estimated uncertainties in the band areas, calculated IR absorption coefficients, and the result obtained using the same procedure to analyze the corresponding region of the Raman spectrum. Computational chemistry (Table 3) reproduces the experimental value fairly well. Depending on the level of approximation used, this value ranges from 2 to 16%. The rest of the normal modes of vibration are listed in Table 1 for the three more abundant forms of FC(O)N=S(O)F₂. The calculations reproduce the experimental wavenumbers well, giving confidence to the analysis of rotational equilibrium, at least for the three more stable forms.

Crystal Structure

Table 2 lists the crystal data for the title compound at 163 K. ((Fluoroformyl)imido)sulfonyl difluoride, FC(O)N=S(O)F₂, crystallizes in the monoclinic space group *P*2₁/*c*, with twelve FC(O)N=S(O)F₂ molecules per unit cell. Of particular interest is the finding that the molecules adopt three similar antiperiplanar–synperiplanar forms **I**, i.e., the more stable form of the isolated molecule on the basis of the calculations and the preferred form in the vapor phase. Only small differences are observed for these three forms (representative differences can reach values up to 0.01 Å for bond distances and 1 and 3° for bond and torsion angles, respectively). The form **I** presents the lowest dipole moment of the series, according to our theoretical calculations (Table 3). It is known that a rotamer with a larger dipole moment is the most likely to be stabilized in the solid state. Consequently, packing effects would appear to either stabilize the forms **I** (Figure 3) in the solid or play a minor role in the case solely because it might eventually favor other forms.

Table 4 lists the experimental dimensions of the more stable forms **I** of FC(O)N=S(O)F₂ illustrated in Figure 3. For the sake of comparison, we also list theoretical dimensions in Table 5.

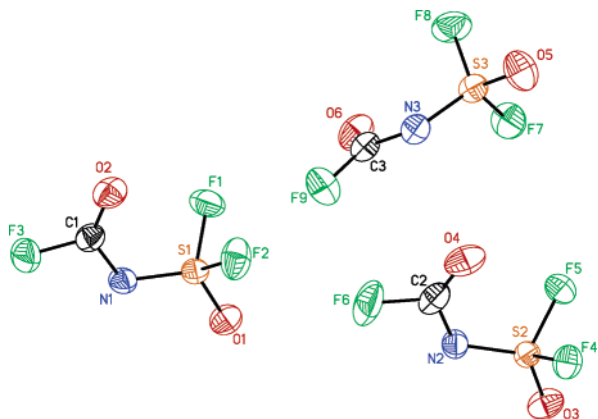
Intermolecular interactions dominated by F⋯F contacts are common for perfluorinated molecules where there is no other choice for stabilizing the packing, e.g., by C–H⋯F–C hydrogen bonds. According to quantum chemical calculations, F⋯F contacts in aromatic systems can contribute up to 14 kcal mol⁻¹ of local stabilization energy.¹³ In the presented case, the three independent molecules are linked by four different contacts (Figures 4 and 5) containing S–F⋯F interactions. The central bond via the inversion

(13) Matta, C. F.; Castillo, N.; Boyd, R. J. *J. Phys. Chem. A* **2005**, *109*, 3669–3681.

Table 3. Calculated Relative Energies (kcal mol⁻¹),^a Relative Abundances at 293 K (%), Wavenumbers (cm⁻¹) of the $\nu(\text{C}=\text{O})$ Mode,^b and Dipole Moments (D) of Stable Forms of $\text{FC}(\text{O})\text{N}=\text{S}(\text{O})\text{F}_2$

form	HF/6-31+G*					B3LYP/6-31+G*					B3LYP/6-311+G*					MP2/6-311+G*				
	ΔE^0	ΔG^0	%	$\tilde{\nu}$	μ	ΔE^0	ΔG^0	%	$\tilde{\nu}$	μ	ΔE^0	ΔG^0	%	$\tilde{\nu}$	μ	ΔE^0	ΔG^0	%	$\tilde{\nu}$	μ
antiperiplanar– synperiplanar (I)	0.00	0.00	80	1842 ^c (589)	1.33	0.00	0.00	72	1868 (428)	1.22	0.00	0.00	69	1871 (451)	1.12	0.00	0.00	70	1872 (400)	1.14
antiperiplanar– antiperiplanar (II)	3.31	2.98	1	1901 ^c (786)	2.69	1.44	1.15	11	1913 (551)	1.97	1.57	1.18	10	1914 (569)	1.71	2.28	1.74	4	1911 (541)	2.09
synclinal– synperiplanar (III)	1.54	0.87	18	1839 (590)	2.72	1.75	1.05	12	1864 (438)	2.17	1.43	0.87	16	1867 (436)	1.93	1.21	0.67	23	1864 (392)	2.22
synclinal– antiperiplanar (IV)	4.32	2.56	1	1898 (811)	3.00	2.81	1.62	5	1916 (592)	2.33	2.68	1.50	5	1918 (615)	2.04	3.10	1.80	3	1915 (578)	2.39

^a Energy differences $\Delta X^0 = X^0(\text{trans-syn}) - X^0(\text{trans-anti})$. Different multiplicities $m = 1$ and $m = 2$ were taken into account. ^b Values between parentheses are IR intensities in km mol⁻¹. ^c Scaled by a factor of 0.9.

**Figure 3.** Molecular structures with atom numbering for $\text{FC}(\text{O})\text{N}=\text{S}(\text{O})\text{F}_2$. Ellipsoids enclose 30% level of probability surfaces.**Table 4.** Experimental and Calculated Geometrical Parameters of Form I of $\text{FC}(\text{O})\text{N}=\text{S}(\text{O})\text{F}_2$ (values in Å and deg)

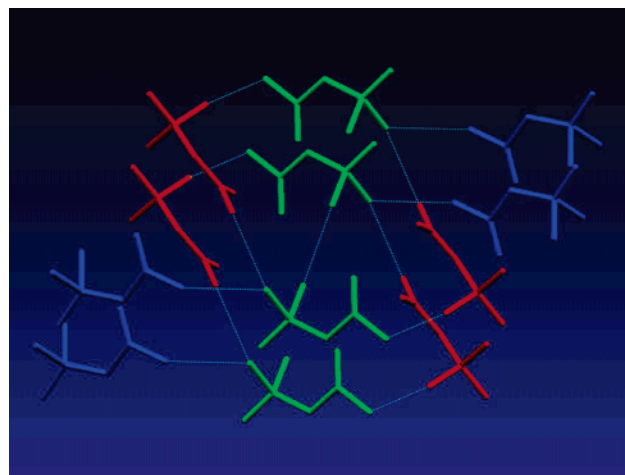
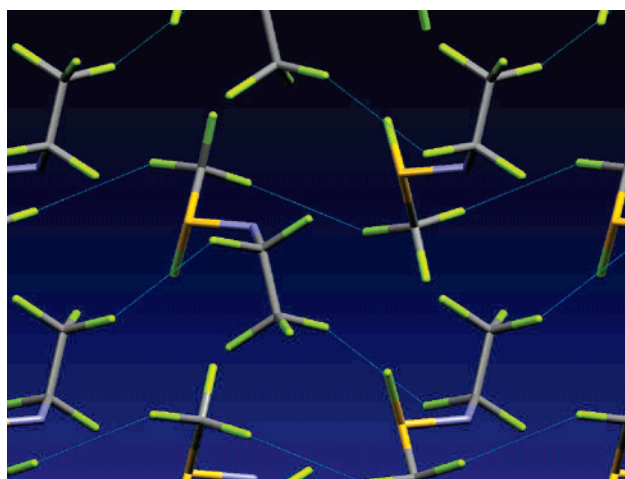
	X-ray ^a	HF/6-31+G*	B3LYP/6-311+G*	MP2/6-311+G*
N=S	1.492(5)	1.488	1.512	1.506
S-F	1.518(12)	1.531	1.600	1.586
C-N	1.378(6)	1.377	1.396	1.400
C=O	1.172(5)	1.174	1.185	1.192
S=O	1.388(2)	1.393	1.423	1.418
C-F	1.332(5)	1.302	1.338	1.333
O-C-N	131.0(3)	128.1	130.2	130.0
F-C-N	107.5(3)	109.0	107.2	107.1
C-N-S	121.0(1)	121.9	122.6	120.8
F-S-F	95.3(4)	95.0	94.5	94.6
F-S-O	109.3(5)	109.1	108.9	108.9
N-S-O	118.0(8)	118.8	118.8	119.4
N-S-F	111.3(5)	111.1	111.5	111.1
F-C-O	121.5(2)	122.2	122.6	123.0

^a Average for the values of the three forms in the solid state.

center has a length of 2.818 Å; the bifurcated bond has lengths of 2.852 and 2.842 Å, and the remaining C-F...F-S contact has a length of 2.881 Å. All these must be considered to be stabilizing contacts, which are in the range of comparative structural studies, in which C-F...F-C contacts at distances of 2.777¹⁴ and 2.868 Å¹⁵ are identified as packing motifs. The F...F van der Waals radius would suggest 2.7 Å as a contact distance, but this obviously does not hold for carbon- or sulfur-bonded fluorine.

(14) Choudhury, A. R.; Urs, U. K.; Guru Row, T. N.; Nagarajan, K. J. *Mol. Struct.* **2002**, *605*, 71–77.

(15) Deepak, C.; Nagarajan, K.; Guru Row, T. N. *Cryst. Growth Des.* **2005**, *5*, 1035–1039.

**Figure 4.** View of the three independent molecules of $\text{FC}(\text{O})\text{N}=\text{S}(\text{O})\text{F}_2$ displayed in different colors. The molecules are linked by $\text{F}\cdots\text{F}$ interactions in the range from 2.82 to 2.88 Å.**Figure 5.** Section of the planar network for $\text{FC}(\text{O})\text{N}=\text{S}(\text{O})\text{F}_2$ consisting of additional $\text{F}\cdots\text{F}$ contacts at a distance of 2.939 Å, viewed perpendicular to (001) using a capped stick model.

Discussion

As mentioned in the Introduction, the molecular structure of $\text{NCNS}(\text{O})\text{F}_2$ ⁵ has already been determined. It exists predominantly in the antiperiplanar (with respect to the S=O double bond and the C-N single bond) form in the gas phase. In the case of $\text{FSO}_2\text{N}=\text{S}(\text{O})\text{F}_2$,¹⁶ the GED pattern

(16) Haist, R.; Alvaréz, R. S. M.; Cutin, E. H.; Della Védova, C. O.; Mack, H.-G.; Oberhammer, H. *J. Mol. Struct.* **1999**, *484*, 249.

Table 5. Comparison of the Experimental Geometrical Parameters for Form **I** of FC(O)N=S(O)F₂ with Related Molecules (values in Å and deg)

	FC(O)NS(O)F ₂ ^a	OSF ₂ ⁷	O ₂ SF ₂ ⁴	HNS(O)F ₂ ⁸	CINS(O)F ₂ ⁹	NCNS(O)F ₂ ⁵	FC(O)NSF ₂ ³	FC(O)NS(F)CF ₃ ⁶	CF ₃ C(O)NS(F)CF ₃ ¹⁰	FC(O)NSCl ₂ ¹¹
N=S	1.4916			1.466(3)	1.484(7)	1.498(12)	1.479(4)	1.549(5)	1.554(8)	1.519(5)
S-F	1.5179	1.5854(2)	1.530(3)	1.549(2)	1.548(3)	1.543(6)	1.586(2)	1.599(4)	1.604(6)	
C-N	1.378					1.34(2)	1.395(6)	1.391(8)	1.392	1.372(20)
C=O	1.172						1.181(4)	1.186(5)	1.200(8)	1.203(6)
S=O	1.3882	1.4127(3)	1.405(3)	1.420(5)	1.394(3)	1.424(5)				
C-F	1.332						1.322(6)	1.331(1)		1.348(6)
O-C-N	131.03						129.3(8)	129.9(12)	129.6(13)	
F-C-N	107.5						106.6(6)	108.2(12)		
C-N-S	120.96						126.7(11)	112.4(11)		
F-S-F	95.27	92.83(2)	96.1(2)	93.7(1)		93.5(13)	93.4(3)		111.2(11)	122.8(17)
F-S-O	109.27	106.82(3)	124.0(2)			107.1(32)				
N-S-O	118.0			119.5(2)		119(2)				
N-S-F	111.34			112.9(1)		113.7(28)	110.4(8)	108.8(33)	112.6	
F-C-O	121.5						124.1(10)	121.9(12)		124.7(17)

^a Average of the values of the three forms.

implies that the vapor at ambient temperatures is made mostly of the antiperiplanar form (with respect to the S=O double bond and the S-N single bond), with a minor contribution from the synperiplanar structure that is not discarded. A similar situation was reported for the related compound CIN=S(O)F₂.⁹ These examples show that N=S(O)F₂-containing compounds present some configurational preference, i.e., a synperiplanar structure may be present in addition to the most abundant antiperiplanar form. The gas-phase configurational composition of FC(O)NS(O)F₂ around the N=S double bond corresponds to the antiperiplanar form in equilibrium with a synclinal structure, whereas similar antiperiplanar forms **I** are found in the solid state, as observed in the present vibrational data and crystal structure.

As noted previously,⁶ the configurational properties of N=S-containing compounds depend primarily on two effects: (i) orbital interactions between the N lone pair and opposite σ^* orbitals (generalized anomeric effect) and (ii) steric repulsions between substituents on nitrogen and sulfur atoms. Steric repulsions would favor a structure with either C-N=S=O or C-N=S-F = 180°. The same preference would be expected for anomeric interactions of the type $n_N \rightarrow \sigma^*$ (SF₂) or $n_N \rightarrow \sigma^*$ (S(O)F). On the other side, the conformational preference of the compound around the C-N bond again implies these two interactions. Although no sensitive steric preference would be expected for synperiplanar or antiperiplanar rotamers, different anomeric interactions of the type $n_N \rightarrow \sigma^*$ (C(O)) in opposition to $n_N \rightarrow \sigma^*$ (CF) would play a role in stabilizing one conformation over the others. Because of the comparable magnitude of both interactions, two conformations are really present in the gas and liquid phases, with the synperiplanar rotamer **I** the most abundant form at room temperature.

A strong anomeric effect would cause shortening of both the S=N and C-N bonds in form **I** of the FC(O)N=S(O)F₂ molecule. For comparing the influence of this stereoelectronic effect on the bond distances, the FC(O)N=S(F)CF₃ results are good candidates. In FC(O)N=S(F)CF₃, steric interactions are stronger than anomeric effects, and thus the antiperiplanar configuration (antiperiplanar with respect to both lone pair orbitals at N and S atoms) is slightly preferred. In this form, orbital interaction no longer causes shortening of the N=S double bond, which is considerably longer (1.549(5) Å) than those in the title compound, structure **I** (1.4952(15),

1.4876(15), and 1.4919(16) Å for the three forms found in the crystal structure). Although a comparison of bond distances for both form **I** of the title compound and FC(O)N=S(F)CF₃ is not straightforward because of the different formal valences at S, and also because different methods of analysis and different phases are used, the C-N values are, as expected, very similar, implying comparable conformational interactions on this part of the molecule. The N=S bond distance for form **I** of the title compound compares quite well with those molecules possessing the -S^{VI}(O)F₂ group, as listed in Table 5. A strong $n_N \rightarrow \sigma^*$ (SF₂) interaction would be reflected, on the other side, in a diminution of the S-F bond order. These distances are very short, as observed in Table 5, showing that the extension of this anomeric interaction is limited. From the same table, a relative short C=O double-bond average distance of 1.172 Å can be observed for FC(O)N=S(O)F₂ in its form **I** as compared to the distances of related molecules, implying no strong anomeric interactions $n_N \rightarrow \sigma^*$ (CF). The C=O double-bond distance was reported as 1.173(2) and 1.172(2) Å for ClC(O)F¹⁷ and OCF₂,¹⁸ respectively. A short S=O double-bond distance is also observed for the title compound, structure **I**, as compared to the distances of related molecules in Table 5. This shortened double bond matches up to CIN=S(O)F₂ more favorably; this implies that certain inductive effects should be present, because the Cl atom electronegativity is comparable with that of the FC(O) group, 3.16 and 2.94, respectively.¹⁹

Conclusion

By using increments of known molecular structures, we can predict the molecular geometry of the most stable form of FC(O)N=S(O)F₂. The structure of the molecule determined in the three phases presents three similar antiperiplanar-synperiplanar forms in the solid state, and a rotameric equilibrium of forms **I**, **II**, **III**, and **IV** in the liquid and gas phases, with **I** being the favored form. Theoretical calculations reproduce the experimental results well.

(17) Oberhammer, H. *J. Chem. Phys.* **1980**, *73*, 4310.

(18) Nakata, M.; Kohata, K.; Fukuyama, T.; Kuchitsu, K.; Wilkins, C. J. *J. Mol. Struct.* **1980**, *68*, 271.

(19) Wu, H. *Zhongguo Kexue Jishu Daxue Xuebao* **1990**, *20* (4), 517.

Experimental Section

Synthesis. The preparation and manipulation of FC(O)N=S(O)-F₂ were carried out in a monel reactor and in an evacuated Pyrex apparatus. Si(NCO)₄ (2.8 g, 14.3 mmol) and SOF₄ (8.7 g, 70 mmol) with BF₃ as catalyst (0.54 g, 8 mmol) were condensed in the reactor, which had previously been dried for 3 h in vacuo (10⁻⁴ Torr) at 70–80 °C. After stirring the reaction mixture at 200 °C for 10 h, we fractionated the volatile components under dynamic vacuum through traps held at -65, -95, and -196 °C.²⁰ The pure compound that collected at -95 °C after repeated condensations was stored in flame-sealed glass ampules under liquid nitrogen in a long-term Dewar vessel. Its melting point is -98 °C.

Instrumentation. (A) X-ray Diffraction at Low Temperature.

An appropriate crystal of FC(O)N=S(O)F₂ ca. 0.3 mm in diameter was obtained on the diffractometer at a temperature of 163(2) K with a miniature zone-melting procedure using focused infrared laser radiation.^{21,22} The diffraction intensities were measured at low temperature on a Nicolet R3m/V four-circle diffractometer. Intensities were collected with graphite-monochromatized Mo K α radiation using the ω -scan technique. The crystallographic data, conditions, and some features of the structure are listed in Table 2. The structure was solved by Patterson syntheses, and refined by the full-matrix least-squares method on F, with the SHELXTL-Plus program.²³ All atoms were assigned to anisotropic thermal parameters. Atomic coordinates, equivalent isotropic displacement coefficients, and anisotropic displacement parameters ($\text{\AA}^2 \times 10^3$) for FC(O)N=S(O)-F₂ are given in the Supporting Information.

(B) Vibrational Spectroscopy. Gas-phase infrared spectra were recorded with a resolution of 1 cm⁻¹ in the range 4000–400 cm⁻¹ on the Bruker IFS 66v FTIR instrument. FT Raman spectra of liquid FC(O)N=S(O)F₂ were recorded with a Bruker RFS 100/S FT Raman spectrometer. The sample in an outside diameter 6 mm glass tube was excited with 150 mW of a 1064 nm Nd:YAG laser (ADLAS, DPY 301, Lübeck, Germany).

(C) NMR Spectroscopy. ¹³C and ¹⁹F NMR spectra were recorded at -45 °C for a CD₃CN solution at room temperature using a 200 MHz Bruker DPX 200 instrument. The ¹³C spectrum consists of a doublet at δ_C 142.1 (FC(O), d, ¹J(CF) = 296.5 Hz). The ¹⁹F spectrum displayed a doublet and singlet with appropriate relative intensities at δ_F +41.97 (SF₂) (SF₂, d, ⁴J(FF) = 9.4 Hz) and +12.86 (FC(O)). Chemical displacements and coupling constants are slightly dependent on the temperature, which can be attributed to distinctive contributions of the single conformers at different temperatures. These data compare fairly well with those reported elsewhere.²⁰

Theoretical Calculations. All the quantum chemical calculations were performed using the GAUSSIAN 98 program package¹² under the Linda parallel execution environment using two coupled PCs. Geometry optimizations were sought with (i) the HF and MP2 approximations and (ii) the B3LYP methods; in all cases, the calculations employed 6-31+G* and 6-311+G* basis sets and standard gradient techniques with simultaneous relaxation of all the geometric parameters.

Acknowledgment. Financial support by the Volkswagen Stiftung (I/78 724) is gratefully acknowledged. The Argentinean authors acknowledge the Fundación Antorchas, Alexander von Humboldt, DAAD (Deutscher Akademischer Austauschdienst, Germany), Agencia Nacional de Promoción Científica y Técnica (ANPCYT), Consejo Nacional de Investigaciones Científicas y Técnicas (CONICET), Comisión de Investigaciones de la Provincia de Buenos Aires (CIC), Facultad de Ciencias Exactas (UNLP), and Universidad Nacional de Tucumán (UNT). C.O.D.V. specially acknowledges the DAAD, which generously sponsors the DAAD Regional Program of Chemistry of the Republic Argentina, supporting Latin-American students earning their Ph.D.s in La Plata.

Supporting Information Available: The crystal data and refinement structure details for the title compound, atomic coordinates, equivalent isotropic displacement parameters, anisotropic displacement parameters, and X-ray crystallographic data in CIF format. This material is available free of charge via the Internet at <http://pubs.acs.org>.

IC050808Q

(20) Ruff, J. K. *Inorg. Chem.* **1966**, *5*, 1787.

(21) Brodalla, D.; Mootz, D.; Boese, R.; Osswald, W. *J. Appl. Crystallogr.* **1985**, *18*, 316.

(22) Boese, R.; Nussbaumer, M. In *Situ Crystallisation Techniques. In Organic Crystal Chemistry*; Jones, D. W., Ed.; Oxford University Press: Oxford, England, 1994; pp 20–37.

(23) *SHELXTL-Plus: A Complex Software Package for Solving, Refining and Displaying Crystal Structures*, version SGI IRIS Indigo; Siemens: Berlin, 1991.